Precipitation over southern Africa: Is there consensus among GCMs, RCMs and observational data?

Maria Chara Karypidou[1], Eleni Katragkou[1], Stefan Pieter Sobolowski[2]

[1] Department of Meteorology and Climatology, School of Geology, Faculty of Sciences, Aristotle University of Thessaloniki, Thessaloniki, Greece
[2] NORCE Norwegian Research Centre, Bjerknes Centre for Climate Research, Bergen, Norway

Correspondence to: karypidou@geo.auth.gr

Abstract. The region of southern Africa (SAF) is highly vulnerable to the impacts of climate change and is projected to experience severe precipitation shortages in the coming decades. Ensuring that our modelling tools are fit for the purpose of assessing these changes is critical. In this work we compare a range of satellite products along with gauge-based datasets. Additionally, we investigate the behaviour of regional climate simulations from the Coordinated Regional Climate Downscaling Experiment (CORDEX) – Africa domain, along with simulations from the Coupled Model Intercomparison Project Phase 5 (CMIP5) and Phase 6 (CMIP6). We identify considerable variability in the standard deviation of precipitation between satellite products that merge with rain gauges and satellite products that do not, during the rainy season (Oct-Mar), indicating high observational uncertainty for specific regions over SAF. Good agreement both in spatial pattern and the strength of the calculated trends is found between satellite and gauge-based products, however. Both CORDEX-Africa and CMIP5 ensembles underestimate the observed trends during the analysis period. The CMIP6 ensemble displayed persistent drying trends, in direct contrast to the observations. The regional ensemble exhibited improved performance compared to its forcing (CMIP5), when the annual cycle and the extreme precipitation indices were examined, confirming the added value of the higher resolution regional climate simulations. The CMIP6 ensemble displayed a similar behaviour to CMIP5, however reducing slightly the ensemble spread. However, we show that reproduction of some key SAF phenomena, like the Angolan Low (which exerts a strong influence on regional precipitation), still poses a challenge for the global and regional models. This is likely a result of the complex climatic process that take place. Improvements in observational networks (both in-situ and satellite), as well as continued advancements in high-resolution modelling will be critical, in order to develop a robust assessment of climate change for southern Africa.

1 Introduction

30   The region of Sub-Saharan Africa has been characterized as one of the most vulnerable regions to climate change (Kula et al., 2013; Serdeczny et al., 2017) and more specifically, the region of southern Africa (SAF) has been identified as a climate change hotspot (Diffenbaugh and Giorgi, 2012). Taking into consideration that the majority of the population living in SAF (70%) is dependent on rainfed agriculture (Mabhaudhi et al., 2018), any climate change induced alteration of the spatiotemporal patterns of precipitation will require a rapid adaptation of the agricultural sector. Concurrently, SAF is also

35   characterized by low adaptive capacity to changes in climatic conditions (Davis and Vincent, 2017), hence, it emerges as a high risk region. In addition, approximately 26% of the SAF population is undernourished (AFDB, 2019). This figure is expected to increase significantly by 2050 (Tirado et al., 2015). Apart from the impacts on the agricultural sector though, climatic changes are expected to alter the spatiotemporal patterns of vector-borne disease occurrence (Rocklöv and Dubrow, 2020), cause severe damage to infrastructure and road networks (Chinowsky et al., 2015) and exacerbate poverty (Azzarri

40   and Signorelli, 2020). Due to these impacts it is critical that the current spatiotemporal patterns of precipitation are accurately reproduced by our modelling systems and observations (whether in-situ, reanalysis or satellite) over SAF. Only then can we credibly assess future climate change impacts and inform strategies aiming to mitigate their effects on local communities.

Towards this end, satellite, gauge-based and reanalysis products are extensively used, in order to monitor current spatial

45   and temporal precipitation patterns and to further characterize precipitation variability and change during recent decades. For future projections however, climate models able to simulate the (thermo)dynamical processes of the atmosphere are employed. Such an endeavor has been performed in the context of the Coupled Model Intercomparison Project Phase 5 (CMIP5) (Taylor et al., 2012) using General Circulation Models (GCMs) and in the context of the Coordinated Regional Climate Downscaling Experiment (CORDEX) – Africa domain (Giorgi and Gutowski, 2015) using Regional Climate

50   Models (RCMs). The latest advancement in the climate modelling community involves GCMs and earth system models (ESMs), participating in the CMIP6 ensemble, providing input for the 6th Assessment Report of the Intergovernmental Panel on Climate Change (IPCC) (Eyring et al., 2016). However, the confidence with which one can claim future climate projections produced by GCMs, ESMs or RCMs are fit for purpose, is usually assessed based on their ability to simulate current climatic conditions. For instance, Munday and Washington (2018) showed that the CMIP5 ensemble displayed a

55   systematic wet bias over the SAF region that was caused by the misrepresentation of orographic features located over the area of Tanzania. A wet bias caused by structural model errors was also identified in the dynamically downscaled and higher-resolution CORDEX-Africa ensemble (Kim et al., 2014). Therefore, a valid question arises as to what the most suitable dataset is, with which climate impact studies can be fed with when the SAF region is concerned. In addition, before the task of characterizing future precipitation trends is addressed, it is imperative to diagnose the degree to which observed

60   precipitation trends over the recent decades are reproduced by GCMs and RCMs.

Satellite and gauge-based datasets display increasing trends (Gu et al., 2016; Harrison et al., 2019) for annual and seasonal precipitation over SAF (32-42 mm year^{-1} per decade), an observation that is also identifiable in the Atmospheric Model Intercomparison Project (AMIP), but not in CMIP5 (Maidment et al., 2015). During DJF, precipitation trends over SAF display a remarkably robust signal in gauge-based, satellite and AMIP datasets (Maidment et al., 2015). In addition,

65 Onyutha (2018) also reported on the increasing precipitation trends over SAF during DJF, especially after the 1960's. However, according to CMIP5, precipitation is projected to decrease over SAF in the 21st century (IPCC, 2013). This estimate also holds for simulations performed using RCMs forced with CMIP5 (Pinto et al., 2016; Dosio et al., 2019). The increase of the observed precipitation trends over SAF has been attributed to the recent strengthening of the Pacific Walker Circulation (PWC) (Maidment et al., 2015), which is captured in observational datasets and in AMIP simulations, but not in

70 CMIP5 (L'Heureux et al., 2013; Yim et al., 2016). CMIP6 displays an even more robust future decline in precipitation and increase of drought events over SAF, relative to its predecessor (Ukkola et al., 2020). However, although the CMIP6 ensemble exhibits multiple improvements on various levels (Wyser et al., 2020), still, certain biases and challenges identified in CMIP5 during the historical period, persist in CMIP6 (Kim et al., 2020).

RCMs are known to add value to climate simulations over regional scales, mainly because the spatial resolution increases,

75 resolving atmospheric waves in a more detailed manner and also, because surface characteristics interacting with the atmosphere are represented more accurately (Denis et al., 2003; Giorgi et al., 2014). Considering the aforementioned challenges displayed in the CMIP5 simulations to accurately capture precipitation amounts under current climatic conditions and recent precipitation trends, we investigate the degree to which this observation holds also for RCMs, forced with GCMs participating in the CMIP5 ensemble. Theory tells us that RCMs develop their own physics. However, often times the impact

80 of the driving GCMs is evident on the RCM simulations (Denis et al., 2003; Laprise et al., 2008; Di Luca et al., 2013; Giorgi, 2019).

Therefore, in this paper we investigate monthly precipitation climatologies and interannual variability and calculate precipitation trends in CMIP5 and CORDEX-Africa simulations, in order to assess whether the CORDEX-Africa ensemble provides any improvement in the simulation of precipitation over the SAF region. We also assess whether the CMIP6

85 ensemble resolves the issues identified in CMIP5. We additionally assess monthly precipitation climatologies and trends in a set of satellite, gauge-based and reanalysis datasets over the SAF region, in order to investigate the level of agreement between the various precipitation products that are often used for precipitation monitoring purposes or evaluation of climate models (Harrison et al., 2019; Alexander et al., 2020). The analysis is performed for the period 1986-2005 over the SAF region.

90 In Section 2 the data used are presented along with the methodology employed. In Section 3 the results are presented and in Section 4 we provide the discussion of the analysis along with some concluding remarks.

2 Data and methodology

2.1 Data

95 We analyse daily and monthly precipitation from 4 types of datasets, namely observational datasets (OBS), GCMs and ESMs that comprise the CMIP5 and CMIP6 ensembles and regional climate models (RCMs) that comprise the CORDEX-Africa ensemble. The analysis is concerned with the SAF region, which is defined as the area between 10 ºE to 42 ºE and 10 ºS to 35 ºS. The analysed period is 1986-2005, as this is the period during which the estimates of all 4 aforementioned datasets overlap. Although satellite and reanalysis products cannot be termed as purely "observational", in the context of the

100 current work they are classified as such, in order to differentiate them from climate model datasets (CORDEX-Africa, CMIP5, CMIP6). Hereafter "OBS" refers to satellite, gauge-based and reanalysis products.

2.1.1 Observational data

The OBS data used are based on the analysis of Le Coz and van de Giesen (2020) and are comprised of 5 gauge-based products (datasets that are derived by spatial interpolation of rain gauges and station data: CRU.v4.01, UDEL.v7,

105 PREC/L.v0.5, GPCC.v7, CPC-Global.v1), 6 satellite products (given below) and 1 reanalysis product, ERA5. The datasets have a temporal coverage that extends through the analysed period (1986-2005). The gauge-based products were chosen so that they have a spatial resolution equal to 0.5º x 0.5º and the satellite products have a spatial resolution less or equal to 0.25º x 0.25º. For satellite products however, there was an exception for 2 products (CMAP.v19.11 and GPCP.v2.2) with a resolution equal to 2.5º x 2.5º that were also included in the analysis due to their wide use in the literature. The OBS

110 ensemble is made of 12 products. More details concerning the OBS datasets are provided in Table S1. In certain parts of the following analysis the OBS products are either used collectively or they are split into sub-ensembles, based on the method(s) used for their production. More specifically, these sub-ensembles are the mean of all gauge-based precipitation products (Gauge-Based), the ensemble mean of satellite products that merge with rain gauges (Satellite-Merge) (ARC.v2, CMAP.v19.11, GPCP.v2.2) and the ensemble mean of satellite products that do not merge directly with rain gauges

115 (Satellite-NoMerge) (CHIRPS.v2, TAMSAT.v3, PERSIANN-CDR), but they use alternative methods such as calibration, bias adjustment or artificial neural network techniques (Le Coz and van de Giesen, 2020).

2.1.2 Climate model simulations

We retrieved daily precipitation for a set of 26 RCM simulations performed as part of CORDEX-Africa historical simulations at 0.44º (~50 km) spatial resolution. In addition, daily precipitation was retrieved for a set of 10 CMIP5 GCMs,

120 with 3 additional simulations with variations in the GCM's resolution (IPSL-LR/IPSL-MR), the ocean model (GFDL-

ESM2M/GFDL-ESM2G) and Realization/Initialization/Physics (ICHCE-EC-EARTH-r1i1p1/ ICHCE-EC-EARTH-r12i1p1). The CMIP5 models selected were the ones used as forcing in the CORDEX-Africa historical simulations. In total, precipitation from a set of 13 CMIP5 simulations was used. Additionally, we exploited daily precipitation from a set of 8 CMIP6 GCM and ESM simulations. The CMIP6 simulations selected were performed with the updated versions of the same

125   models that were part of the CMIP5 ensemble. This selection served to construct CMIP5 and CMIP6 ensembles that were comparable. Precipitation data for all simulations were retrieved from the Earth System Grid Federation (ESGF). In addition, we retrieved temperature at 850 hPa for the CORDEX-Africa from ESGF. For the CMIP5 simulations temperature at 850 hPa was retrieved from the Climate Data Store (CDS). Temperature at 850 hPa was not available for CMIP6, hence the CMIP6 ensemble is not included in the analysis employing temperature at 850 hPa. Lastly, elevation data for CORDEX-

130   Africa and CMIP5 were obtained from ESGF, while the Shuttle Radar Topography Mission (SRTM) (Farr et al., 2007) Digital Elevation Model was used as the observed elevation in the topography transects for a selected latitude over SAF. Details about the models used are provided in Tables S2-S4.

2.2 Methodology

135   Precipitation climatologies are investigated on a monthly basis, due to the fact that precipitation over SAF arises as the result of atmospheric mechanisms that display high variability during the rainy season. The aggregation of precipitation to seasonal means might often obscure certain spatial characteristics that are better identified on a monthly basis. The within-ensemble agreement is investigated using the sample standard deviation (SD). We also employ 4 precipitation indices constructed in the context of the Expert Team on Climate Change Detection and Indices (ETCCDI) (Peterson and Manton,

140   2008), utilising daily precipitation amounts for the period 1986-2005. The 4 ETCCDI indices are used to describe total annual precipitation (PRCPTOT), annual maximum daily precipitation (Rx1Day), annual number of days with daily precipitation >10 mm (R10mm) and annual number of days with daily precipitation >20 mm (R20mm). These indices are calculated for each individual simulation (CMIP5, CMIP6 and CORDEX), and OBS product, separately and yield a value for every year (Jan – Dec) during the period 1986-2005. The calculation of indices required data having a daily temporal

145   resolution, hence, observational datasets that provided monthly aggregates are excluded. The spatial averages calculated over SAF for the annual cycle and the ETCCDI indices consider land pixels only. For the construction of ensemble means, either in observational or model ensembles, datasets were remapped to the coarser grid using conservative remapping for precipitation and bilinear interpolation for temperature at 850 hPa.

In order to investigate some basic thermodynamical aspects that may differentiate precipitation in the CMIP5 and the

150   CORDEX-Africa ensembles, we look into the seasonal representation of the Angola low (AL) pressure system over SAF. The AL pressure system is a semi-permanent synoptic scale system, that plays a strong role in modulating precipitation over SAF (Reason and Jagadheesha, 2005; Lyon and Mason, 2007; Crétat et al., 2019; Munday and Washington, 2017; Howard

and Washington, 2018). In the current work, we use potential temperature at 850 hPa (theta850), as an indication of the strength of the AL pressure system over the SAF region. Potential temperature at 850 hPa is calculated using Poisson's

155   equation (https://glossary.ametsoc.org/wiki/Poisson_equation).

Lastly, the Theil-Sen's slope (Theil, 1992; Sen, 1968) for monthly precipitation during the period 1986-2005 is calculated for each dataset. This is a non-parametric approach to estimate trends, that is insensitive to outliers. Statistical significance is assessed using the Mann-Kendall test (Mann, 1945; Kendall, 1948).

3 Results

160   ### 3.1 Climatology

Figure 1 displays monthly precipitation climatologies during Oct-Mar (rainy season over the study region) for ERA5 and for the ensemble means of 6 additional types of datasets. At the beginning of the rainy season (Oct) all products display precipitation maxima at the north-western part of the study region. Another precipitation maxima is observed at eastern South Africa. For both regions, there is a slight tendency for gauge-based products to yield approximately 1 mm d^{-1} less

165   precipitation than reanalysis and satellite products. The CMIP5, CMIP6 and CORDEX-Africa ensembles are also in agreement with regards to the location and amounts, however, CORDEX-Africa displays approximately 2 mm d^{-1} more precipitation over Angola. During November, the rainband extends southwards and the region over South Africa experiencing high precipitation enlarges.

Moving towards the core of the rainy season (DJF) the precipitation maxima extends southwards following the collapse

170   of the congo air boundary (CAB) (Howard and Washington, 2019) and high precipitation amounts are also observed over the eastern part of the study region. More specifically, during January high precipitation amounts (>10 mm d^{-1}) are observed over an extended region in northern Mozambique for non-merging satellite products (Satellite-NoMerge). This area is also identified as a region of high precipitation in gauge-based products and in merging satellite products, however, with a smaller magnitude. In ERA5, the spatial pattern of precipitation is more patchy and exhibits higher than observed

175   precipitation amounts in the wider region of lake Malawi, reaching extremely high values (34 mm d^{-1}), as also indicated in the known precipitation issues of ERA5 over Africa (Hersbach et al., 2020). During DJF the CORDEX-Africa ensemble displays precipitation values >3 mm d^{-1} over almost all of the SAF region. This observation is also consistent in CMIP5 and CMIP6, however, maximum precipitation amounts in CMIP5 and CMIP6 are approximately >3 mm d^{-1} larger than in the CORDEX-Africa ensemble. In March, the rainband starts its northward shift, nevertheless, high precipitation amounts are

180   still observed over the eastern parts of the study region and over the coastal region of Angola. The retreat of the rainband is evident in CORDEX-Africa, however, CMIP5 and CMIP6 still exhibit extended regions of high precipitation.

In Fig. 2 SD values for the 6 ensembles is presented during months Oct-Mar for the period 1986-2005 expressed as mm d^{-1} and is used as a measure of the within-ensemble agreement. As it is shown for gauge-based products, during October and

November high SD values are observed primarily over Angola. For months Dec-Mar Angola remains a high SD region, however, increased SD values are also observed over the eastern parts of the study region and especially over northern Mozambique. An important aspect influencing gauge-based products is the spatiotemporal coverage of the rain gauges used (Le Coz and van de Giesen, 2020), which is highly variable between regions and reporting periods. More specifically, after the 1970's the rain gauge coverage over Africa has decreased significantly (Janowiak, 1988) and the gauge network has been particularly sparse over the SAF region (Lorenz and Kunstmann, 2012; Giesen et al., 2014), which further implies that gauge-based products depend on extrapolating values from surrounding gauges. Therefore, station density and the interpolation method employed are key factors in determining the accuracy of the final product (Le Coz and van de Giesen, 2020). The high SD values over Angola, are mainly due to the scarcity of available rain gauges used in the interpolation method (Fig. S1). After 1995, there is a noticeable reduction of the station/rain gauge data used over the SAF region (Fig. S2) for 3 of the gauge-based products.

A similar spatiotemporal pattern of SD is also observed in satellite-based products (Satellite-Merge) which employ algorithms that merge rain gauges with thermal-infrared (TIR) images. This is indicative of the strong impact that the location and number of rain gauges exert on satellite algorithms that employ merging techniques (Maidment et al., 2014, 2015). The spatiotemporal pattern of SD for satellite-based products that do not merge with gauges (Satellite-NoMerge) displays low SD values for October and November, however, during DJF localized areas of high SD appear over Angola, Zambia, Malawi and Mozambique. The satellite products used in this ensemble are based on TIR images and precipitation is indirectly assessed through cloud top temperature (Tarnavsky et al., 2014; Ashouri et al., 2015; Funk et al., 2015). Hence, the occurrence and severity of precipitation is calculated based on a temperature threshold. In cases that the threshold is set to very low cloud top temperature values, the algorithm has high skill at identifying deep convection, however, warm rain events are not adequately captured (Toté et al., 2015). As it is shown in Fig. 2, high SD values in non-merging satellite products are primarily observed over coastal regions and over regions where the elevation increases rapidly. These type of regions can be associated with orographic or frontal lifting of air masses (Houze, 2012), resulting in precipitation, without the threshold temperature of the cloud top being reached.

In the CORDEX-Africa ensemble SD values are >0.8 mm d⁻¹ over almost all of the SAF region, however, very high SD values (3-9.8 mm d⁻¹) are observed in the coastal part of Angola and over the lake Malawi region during Nov-Mar. In the CMIP5 ensemble the spatiotemporal pattern of SD values exceeds 2 mm d⁻¹ during Nov-Mar throughout the whole SAF region. CMIP6 displays a similar SD pattern. During March however, CMIP6 displays a substantial improvement in the agreement between its ensemble members. Overall, for the whole extent of SAF, the CORDEX-Africa ensemble displays greater agreement among ensemble members, however SD values become large over specific localized regions at western Angola and in the Malawi region. The CMIP5 and CMIP6 ensembles although not displaying the localized extreme SD values as CORDEX-Africa, displays generally high SD values throughout the whole extent of SAF.

3.2 Annual cycle

Figure 3 displays the annual cycle of precipitation in the CORDEX-Africa, CMIP5, CMIP6 and observational ensembles for land grid points. All datasets capture the unimodal distribution of precipitation over SAF, however considerable differences in precipitation amount and spread are observed.

220   Specifically, the CMIP5 ensemble exhibits significantly higher precipitation amounts than the CORDEX-Africa and observational ensembles. This difference becomes particularly pronounced during the rainy season, with CMIP5 yielding approximately 2 mm d^{-1} more precipitation than the observational ensemble. It is also notable that for Nov-Feb, even the driest ensemble members of CMIP5 yield approximately 1 mm d^{-1} more precipitation than the wettest ensemble members of the observational data. This is in agreement with Munday and Washington (2018) who identified a systematic wet bias over

225   SAF in CMIP5, that was associated with an intensified north-easterly transport of moisture that erroneously reaches SAF, due to the poorly represented orography in the region of Tanzania and Malawi (which would hinder moisture originating from the Indian ocean from reaching SAF and instead force it to recurve towards the region of Madagascar). The behaviour of CMIP6 is similar to CMIP5, with a slightly smaller ensemble spread during Jan-Mar and a considerable reduction in spread during November.

230   The CORDEX-Africa ensemble reduces precipitation amounts during the core of the rainy season (DJF) compared to CMIP5, however, its behavior during the rest of the months is complicated. More specifically, during Aug-Oct CORDEX-Africa displays slightly higher precipitation amounts compared to CMIP5. During November, the difference between the CORDEX-Africa and the CMIP5 ensembles becomes noticeable, with the CMIP5 ensemble mean becoming 0.4 mm d^{-1} larger than the CORDEX-Africa ensemble mean. During DJF the differences between the 2 ensembles maximize, with the

235   CORDEX-Africa ensemble displaying good agreement with the OBS ensemble (<1 mm d^{-1} difference in the ensemble means of CORDEX-Africa and OBS). From March until July, the difference between the CORDEX-Africa and CMIP5 ensembles starts to reduce gradually. Since the maximum impact of the north-easterly moisture transport into SAF responsible for the wet bias in CMIP5 occurs during DJF (Munday and Washington, 2018), the impact of the CORDEX-Africa increase in resolution and the effect of the improved representation of topography is also more intensely identified

240   during DJF. As it is displayed in Fig. 4, surface orography is substantially improved in the CORDEX-Africa ensemble, relative to CMIP5.

     During the wet season (Oct-Mar) the spread within the members of each ensemble maximizes and is particularly large for CMIP5 (approximately 2 mm d^{-1}). In CORDEX-Africa the ensemble spread reaches 1 mm/d during the rainy season, while for the observational ensemble the spread is <0.5 mm d^{-1}. Overall, both CMIP5 and CORDEX-Africa ensembles capture the

245   seasonal cycle of precipitation over SAF, however, CORDEX-Africa displays a substantial improvement with regards to precipitation amounts and spread.

3.3 Angola low

In Fig. 5 the annual cycle of theta850 for the CMIP5 and CORDEX-Africa ensembles and for ERA5 is displayed. In the current work, theta850 is used as an indication of the strength of the AL pressure system that is identified as one of the major

250 mechanisms modulating precipitation over the SAF region. During the rainy season (Oct-Mar) the CORDEX-Africa ensemble displays lower values, with larger uncertainty, compared to the CMIP5 ensemble. Both RCM and GCM ensembles, display lower theta850 values throughout the year, relative to ERA5. Taking into consideration the association between precipitation and the strength of the AL, we can deduce that the AL has a weaker representation in the CORDEX-Africa ensemble, relative to CMIP5. This is also captured in Fig. S3, where potential temperature differences at 850 hPa

255 from ERA5 are displayed for the CORDEX-Africa ensemble (CORDEX-Africa – ERA5) and for the CMIP5 ensemble (CMIP5 – ERA5). Values refer to the monthly climatological mean differences, for the period 1986-2005. The regions of maximum heating at 850 hPa are displayed in Fig. S4. Both ensembles display the southward migration of the area of maximum heating during the rainy season, following the seasonal cycle of the AL pressure system (Munday and Washington, 2017). The region of maximum heating in both intensity and extent is observed during Oct-Nov for both the

260 CORDEX-Africa and the CMIP5 ensembles, when the AL is primarily a heat low, while during Dec-Feb it acquires tropical low characteristics (Howard and Washington, 2018).

The fact that the CORDEX-Africa ensemble displays lower values of potential temperature at 850 hPa relative to CMIP5, may partly explain why the CORDEX-Africa ensemble displays lower monthly precipitation values than the CMIP5 ensemble, at least over this region.

265 ### 3.4 Precipitation indices

Total annual precipitation (PRCPTOT) is displayed in Fig. 6 (a). The mean of the CMIP5 ensemble displays the largest amounts of PRCPTOT (approximately 1000 mm year^{-1}). The CORDEX-Africa ensemble systematically reduces this amount by approximately 200 mm year^{-1}, yielding PRCPTOT values closer to that of the observational datasets. Both CMIP5 and CORDEX-Africa display similar within-ensemble variability. The ensemble mean of the observational datasets is

270 considerably lower than CORDEX-Africa and it displays an interannual variability between 500-800 mm year^{-1}. Both the ensemble means of CMIP5 and CORDEX-Africa fail to reproduce the interannual variability of the observational ensemble. The ensemble mean in CMIP6 is comparable to CMIP5, however, CMIP6 displays more distinct interannual variability. In Fig. 6 (b) the annual maximum 1 day precipitation (Rx1Day) is displayed. For Rx1Day, the mean of the CMIP5 ensemble is in close agreement with the mean of the observational ensemble (approximately 40 mm d^{-1}). The ensemble mean of

275 CORDEX-Africa yields larger precipitation amounts (approximately 55 mm d^{-1}) than CMIP5 and the observational ensemble. As it is shown in Fig. 6 (b), the CORDEX-Africa ensemble mean is influenced by higher Rx1Day values, originating from ensemble members that cluster within the range 65-85 mm d^{-1}. The spread of the CMIP5 ensemble is comparable to that of the observational data, however, the CORDEX-Africa ensemble spread is still larger, ranging from 25-

85 mm d^{-1}. The CMIP6 ensemble falls between the CORDEX-Africa and CMIP5 ensembles, with a spread comparable to

280 that of CMIP5. In Fig. 6 (c) the annual number of days with daily precipitation greater than 10 mm (R10mm) is presented. It is noted that the ensemble mean of the CORDEX-Africa ensemble is closer to that of the observational datasets (20-25 days year^{-1} with daily precipitation greater than 10 mm). The mean of the CMIP5 ensemble yields approximately 34 days of extreme precipitation annually. It is also highlighted that the CMIP5 ensemble displays a large range of R10mm values (10-55 days year^{-1}). Again, the CMIP6 ensemble mean coincides with that of CMIP5, however, displaying a smaller ensemble

285 spread. In Fig. 6 (d) the annual number of days with daily precipitation greater than 20 mm (R20mm) is shown. There is close agreement between the CMIP5 and CORDEX-Africa ensembles, however both datasets overestimate R20mm relative to the observational data. Again, the CMIP5 ensemble displays the largest spread and a very weak interannual variability is seen on both CMIP5 and CORDEX-Africa ensemble means. The CMIP6 ensemble mean is slightly greater than its predecessor.

290 **3.5 Trends**

In Fig. 7 the monthly precipitation trends for the rainy season of the period 1986-2005 are displayed for all 3 observational data (gauge-based, SatelliteMerge Satellite-NoMerge) and for the CORDEX-Africa, CMIP5 and CMIP6 ensembles. Precipitation trends display considerable agreement among all 3 observational datasets, both concerning the signal and the magnitude of the trend. However, the CORDEX-Africa and CMIP5 ensembles display trends that are

295 considerably smaller in magnitude. In addition, CORDEX-Africa, CMIP5 and CMIP6 ensembles display fairly distinct spatial patterns that are not in agreement either among them, or with the spatial pattern of precipitation trends displayed by the observational datasets,

More specifically, during October, all observational products display decreasing trends for the most part of SAF that reach up to -0.1 mm d^{-1} per 20 years. During November the signal changes and SAF experiences increasing trends, with an

300 exception for NW SAF, northern Mozambique and regions of eastern South Africa. During December increasing trends become even more spatially extended and pronounced, especially for satellite products. During January, certain areas of decreasing trends over northern SAF appear, while during February decreasing trends are observed over almost the whole extent of SAF. In March, increasing trends are observed in the region extending from southern Mozambique and stretching towards Zimbabwe and southern Zambia.

305 Monthly precipitation trends in the CORDEX-Africa ensemble are significantly weaker than in the observational datasets and display precipitation increase during Oct–Dec. After January certain regions of intensified decreasing trends appear over southern Angola-northern Namibia and Botswana (Jan) and over Botswana and South Africa (Feb). In CMIP5 decreasing trends are observed during October, but for November increasing trends are observed over the northern part of SAF. During December, strong increasing trends (0.1 mm d^{-1} per 20 years) appear for central SAF, however, during January almost all of

310 the SAF region (with an exception for Mozambique) experiences decreasing precipitation trends. In CMIP6 persistent drying trends are observed almost throughout the whole of SAF and are particularly strong during Jan-Feb (-0.1 mm d^{-1} per 20

years). During March however, the signal is reversed. Statistical significance assessed with the Mann-Kendall test is shown in Fig. S5.

4 Discussion and conclusions

315 The analysis of the SD among the different observational products highlights the fact that precipitation assessment requires consultation of multiple (gauge-based, satellite or reanalysis) products. If this is not possible, then it is highly recommended that the spatial distribution and frequency of reporting of the underlying station data is examined, for each respective precipitation product in use. This should be also regarded in cases when gauge-based or satellite products are utilized for model evaluation purposes. Moreover, satellite products that merge with rain gauges should not be considered independent

320 from gauge-based products that exploit similar gauge-networks. In addition, we note that SD in the CORDEX-Africa ensemble is considerably lower than in the CMIP5/6 ensembles, supplying evidence that the CORDEX-Africa set of simulations provide more constrained results and can thus be considered to be a suitable dataset for climate impact assessment studies over SAF.

Concerning the annual cycle of precipitation, we note that although the seasonality is captured reasonably by both the

325 CMIP and CORDEX-Africa ensembles, still, there are considerable differences between the two. More specifically, we conclude that the CORDEX-Africa ensemble exhibits smaller ensemble spread for all months of the rainy season compared to the driving GCMs (CMIP5). We also conclude that the strong wet bias over SAF in the CMIP5 ensemble (Munday and Washington, 2018) is considerably reduced in the CORDEX-Africa ensemble. This bias is still evident in CMIP6. A plethora of references in the literature (Reason and Jagadheesha, 2005; Lyon and Mason, 2007; Crétat et al., 2019; Munday and

330 Washington, 2017; Howard and Washington, 2018) have highlighted the importance of the AL pressure system in modulating precipitation over SAF. We note that the strength of the AL as assessed in the current study was simulated to be weaker in the CORDEX-Africa than in the CMIP5 ensemble. This may partly explain why precipitation in the CORDEX-Africa ensemble is reduced, relative to the CMIP5 ensemble. However, there is need for a more in-depth dynamical analysis of the simulation of the AL in the CORDEX-Africa ensemble and its impact on modulating precipitation seasonality and

335 patterns over SAF.

The use of the 4 ETCCDI indices demonstrated that the CORDEX-Africa ensemble yields results that are in closer agreement to the observational data, compared to CMIP5/6 ensembles. It is, nevertheless, noticed that the improvement in the CORDEX-Africa ensemble is most evident when the ensemble mean is used. This highlights the fact that the ensemble mean performance is improved, relative to the performance of individual models (Nikulin et al., 2012). For this reason, it is

340 advisable that climate impact studies employ multi-model ensemble means, as a method of obtaining the consensus climatic information emanating from various models (Duan et al., 2019). In addition, we underline the fact that in all indices the ensemble means of CMIP5 and CORDEX-Africa were not able to reproduce the interannual variability that was seen in the observational ensemble. This remark is in agreement with the fact that the task of reproducing precipitation variability across

various time-scales by the CMIP5 ensemble is known to present challenges (Dieppois et al., 2019), that inevitably cascade
345 into the CORDEX-Africa simulations that are forced with CMIP5 GCMs (Dosio et al., 2015). Lastly, despite the fact that the
CORDEX-Africa ensemble reduces precipitation amounts over SAF, its use in drought-related impact studies should take
into consideration that still, it yields larger precipitation amounts than the observational data, which might eventually lead to
underestimation of drought risk.

Precipitation trends during the rainy season displayed high spatial variability depending on the month. All observed
350 (gauge-based and satellite) trends display substantial spatial agreement. The precipitation trends obtained by the CMIP5/6,
and CORDEX-Africa ensembles, did not display consistency with the trends obtained from the observational datasets. This
is not entirely unexpected, due to the role of internal variability compared to external forcing in recent decades (Pierce et al.,
2009), unlike temperature trends which have been shown to have a good agreement between the CORDEX-Africa and
CMIP5 ensembles with observed temperature trends (Dosio and Panitz, 2016; Warnatzsch and Reay, 2019).

355 In conclusion, while CORDEX-Africa displays marked improvement over coarser resolution products, there are still
improvements to be made. In the world of regional climate modelling community, the 0.44° resolution of CORDEX-Africa is
no longer state of the art and ensemble efforts are now approaching convection permitting grid-spacing (i.e., < 4 km) in some
parts of the world (Ban et al., 2021; Pichelli et al., 2021). The next generation ensembles for Africa will be around 0.22°
degree and will hopefully provide insight and improvements to the challenges described here.

360

Code and data availability

Analysis was performed using the R Project for Statistical Computing (https://www.r-project.org/), the Climate Data
Operators (CDO) (https://code.mpimet.mpg.de/projects/cdo/) and Bash programming routines. Processing scripts are
available via ZENODO under DOI: https://doi.org/10.5281/zenodo.4725441. CMIP5, CMIP6 and CORDEX-Africa daily
365 precipitation data were retrieved from the Earth System Grid Federation (ESGF) portal (https://esgf-data.dkrz.de/projects/esgf-dkrz/). CMIP5 temperature data at 850 hPa were retrieved from the Climate Data Store (CDS)
(https://cds.climate.copernicus.eu/#!/home). CORDEX-Africa temperature data at 850 hPa were retrieved from ESGF.
Surface elevation data for CMIP5 and CORDEX-Africa were retrieved from ESGF. The Shuttle Radar Topography Mission
(SRTM) Digital Elevation Model was retrieved from: https://srtm.csi.cgiar.org/. ERA5 data were retrieved from CDS.
370 Climate Research Unit (CRU) data are available at: https://crudata.uea.ac.uk/cru/data/hrg/. The University of Delaware
(UDEL) data are available at: https://psl.noaa.gov/data/gridded/data.UDel_AirT_Precip.html. The CPC Global Unified
Gauge-Based Analysis of Daily Precipitation (CPC-Unified) was retrieved from:
https://psl.noaa.gov/data/gridded/data.cpc.globalprecip.html. NOAA's PRECipitation REConstruction over Land dataset
(PREC/L) was retrieved from: https://psl.noaa.gov/data/gridded/data.precl.html. The dataset of the Global Precipitation
375 Climatology Centre (GPCC) was retrieved from: https://psl.noaa.gov/data/gridded/data.gpcc.html. The Tropical Applications
of Meteorology using SATellite (TAMSAT) data were retrieved from: http://www.tamsat.org.uk/. The Precipitation

Estimation from Remotely Sensed Information using Artificial Neural Networks – Climate Data Record (PERSIANN-CDR) are available at: https://chrsdata.eng.uci.edu/. The Climate Hazards Group InfraRed Precipitation with Station data (CHIRPS) products are available at: https://www.chc.ucsb.edu/data/chirps. The CPC Merged Analysis of Precipitation 380 (CMAP) dataset was retrieved from: https://psl.noaa.gov/data/gridded/data.cmap.html. The Global Climatology Precipitation Project (GPCP) dataset was retrieved from: https://psl.noaa.gov/data/gridded/data.gpcp.html. The African Rainfall Climatology (ARC) dataset is available at: https://iridl.ldeo.columbia.edu/SOURCES/.NOAA/.NCEP/.CPC/.FEWS/.Africa/.DAILY/.ARC2/.daily/index.html?Set-Language=en.

385

Supplement

The supplement related to this article is available online.

Author contribution

390 MCK, EK and SPS designed the research. MCK implemented the analysis and prepared the manuscript. EK and SPS editted the manuscript and provided corrections.

Competing interests

The authors declare that they have no competing interests.

395

Acknowledgements

MCK was funded by the Hellenic Foundation for Research & Innovations, under the 2nd Call for PhD Candidates (application No. 1323). This article is funded by the AfriCultuReS project "Enhancing Food Security in African Agricultural Systems with the Support of Remote Sensing", (European Union's Horizon 2020 Research and Innovation Framework 400 Programme under grant agreement No. 774652). The authors would like to thank the Scientific Support Centre of the Aristotle University of Thessaloniki (Greece) for providing computational/storage infrastructure and technical support.

References

AFDB, 2019. Southern Africa Economic Outlook 2019. African Development Bank.

Alexander, L.V., Bador, M., Roca, R., Contractor, S., Donat, M.G., Nguyen, P.L., 2020. Intercomparison of annual
405   precipitation indices and extremes over global land areas from in situ, space-based and reanalysis products.
         Environ. Res. Lett. 15, 055002. https://doi.org/10.1088/1748-9326/ab79e2

Ashouri, H., Hsu, K.-L., Sorooshian, S., Braithwaite, D.K., Knapp, K.R., Cecil, L.D., Nelson, B.R., Prat, O.P., 2015.
         PERSIANN-CDR: Daily Precipitation Climate Data Record from Multisatellite Observations for Hydrological and
         Climate Studies. Bull. Am. Meteorol. Soc. 96, 69–83. https://doi.org/10.1175/BAMS-D-13-00068.1

410 Azzarri, C., Signorelli, S., 2020. Climate and poverty in Africa South of the Sahara. World Dev. 125, 104691.
         https://doi.org/10.1016/j.worlddev.2019.104691

Ban, N., Caillaud, C., Coppola, E., Pichelli, E., Sobolowski, S., Adinolfi, M., Ahrens, B., Alias, A., Anders, I., Bastin, S.,
         Belusic, D., Berthou, S., Brisson, E., Cardoso, R.M., Chan, S., Christensen, O.B., Fernandez, J., Fita, L., Frisius, T.,
         Gasparac, G., Giorgi, F., Goergen, K., Haugen, J.E., Hodnebrog, O., Kartsios, S., Katragkou, E., Kendon, E.J.,
415   Keuler, K., Lavin-Gullon, A., Lenderink, G., Leutwyler, D., Lorenz, T., Maraun, D., Mercogliano, P., Milovac, J.,
         Panitz, H.-J., Raffa, M., Remedio, A.R., Schar, C., Soares, P.M.M., Srnec, L., Steensen, B.M., Stocchi, P., Tolle,
         M.H., Truhetz, H., Vergara-Temprado, J., de Vries, H., Warrach-Sagi, K., Wulfmeyer, V., Zander, M., 2021. The
         first multi-model ensemble of regional climate simulations at the kilometer-scale resolution, Part I: Evaluation of
         precipitation. Clim Dynamics.

420 Chinowsky, P.S., Schweikert, A.E., Strzepek, N.L., Strzepek, K., 2015. Infrastructure and climate change: a study of impacts
         and adaptations in Malawi, Mozambique, and Zambia. Clim. Change 130, 49–62. https://doi.org/10.1007/s10584-
         014-1219-8

Crétat, J., Pohl, B., Dieppois, B., Berthou, S., Pergaud, J., 2019. The Angola Low: relationship with southern African rainfall
         and ENSO. Clim. Dyn. 52, 1783–1803. https://doi.org/10.1007/s00382-018-4222-3

425 Davis, C.L., Vincent, K., 2017. Climate risk and vulnerability: A handbook for Southern Africa. CSIR.

Denis, B., Laprise, R., Caya, D., 2003a. Sensitivity of a regional climate model to the resolution of the lateral boundary
         conditions. Clim. Dyn. 20, 107–126. https://doi.org/10.1007/s00382-002-0264-6

Denis, B., Laprise, R., Caya, D., 2003b. Sensitivity of a regional climate model to the resolution of the lateral boundary
         conditions. Clim. Dyn. 20, 107–126. https://doi.org/10.1007/s00382-002-0264-6

430 Di Luca, A., de Elía, R., Laprise, R., 2013. Potential for added value in temperature simulated by high-resolution nested
         RCMs in present climate and in the climate change signal. Clim. Dyn. 40, 443–464. https://doi.org/10.1007/s00382-
         012-1384-2

Dieppois, B., Pohl, B., Crétat, J., Eden, J., Sidibe, M., New, M., Rouault, M., Lawler, D., 2019. Southern African summer-
         rainfall variability, and its teleconnections, on interannual to interdecadal timescales in CMIP5 models. Clim. Dyn.
435   53, 3505–3527. https://doi.org/10.1007/s00382-019-04720-5

Diffenbaugh, N.S., Giorgi, F., 2012. Climate change hotspots in the CMIP5 global climate model ensemble. Clim. Change
         114, 813–822. https://doi.org/10.1007/s10584-012-0570-x

Dosio, A., Jones, R.G., Jack, C., Lennard, C., Nikulin, G., Hewitson, B., 2019. What can we know about future precipitation
         in Africa? Robustness, significance and added value of projections from a large ensemble of regional climate
440   models. Clim. Dyn. 53, 5833–5858. https://doi.org/10.1007/s00382-019-04900-3

Dosio, A., Panitz, H.-J., 2016. Climate change projections for CORDEX-Africa with COSMO-CLM regional climate model
         and differences with the driving global climate models. Clim. Dyn. 46, 1599–1625. https://doi.org/10.1007/s00382-
         015-2664-4

Dosio, A., Panitz, H.-J., Schubert-Frisius, M., Lüthi, D., 2015. Dynamical downscaling of CMIP5 global circulation models
445   over CORDEX-Africa with COSMO-CLM: evaluation over the present climate and analysis of the added value.
         Clim. Dyn. 44, 2637–2661. https://doi.org/10.1007/s00382-014-2262-x

Duan, H., Zhang, G., Wang, S., Fan, Y., 2019. Robust climate change research: a review on multi-model analysis. Environ.
         Res. Lett. 14, 033001. https://doi.org/10.1088/1748-9326/aaf8f9

Eyring, V., Bony, S., Meehl, G.A., Senior, C.A., Stevens, B., Stouffer, R.J., Taylor, K.E., 2016. Overview of the Coupled
450   Model Intercomparison Project Phase 6 (CMIP6) experimental design and organization. Geosci. Model Dev. 9,
         1937–1958. https://doi.org/10.5194/gmd-9-1937-2016

Farr, T.G., Rosen, P.A., Caro, E., Crippen, R., Duren, R., Hensley, S., Kobrick, M., Paller, M., Rodriguez, E., Roth, L., Seal, D., Shaffer, S., Shimada, J., Umland, J., Werner, M., Oskin, M., Burbank, D., Alsdorf, D., 2007. The Shuttle Radar Topography Mission. Rev. Geophys. 45. https://doi.org/10.1029/2005RG000183

455 Funk, C., Peterson, P., Landsfeld, M., Pedreros, D., Verdin, J., Shukla, S., Husak, G., Rowland, J., Harrison, L., Hoell, A., Michaelsen, J., 2015. The climate hazards infrared precipitation with stations—a new environmental record for monitoring extremes. Sci. Data 2, 150066. https://doi.org/10.1038/sdata.2015.66

Giesen, N. van de, Hut, R., Selker, J., 2014. The Trans-African Hydro-Meteorological Observatory (TAHMO). WIREs Water 1, 341–348. https://doi.org/10.1002/wat2.1034

460 Giorgi, F., 2019. Thirty Years of Regional Climate Modeling: Where Are We and Where Are We Going next? J. Geophys. Res. Atmospheres 124, 5696–5723. https://doi.org/10.1029/2018JD030094

Giorgi, F., Coppola, E., Raffaele, F., Diro, G.T., Fuentes-Franco, R., Giuliani, G., Mamgain, A., Llopart, M.P., Mariotti, L., Torma, C., 2014. Changes in extremes and hydroclimatic regimes in the CREMA ensemble projections. Clim. Change 125, 39–51. https://doi.org/10.1007/s10584-014-1117-0

465 Giorgi, F., Gutowski, W.J., 2015. Regional Dynamical Downscaling and the CORDEX Initiative. Annu. Rev. Environ. Resour. 40, 467–490. https://doi.org/10.1146/annurev-environ-102014-021217

Gu, G., Adler, R.F., Huffman, G.J., 2016. Long-term changes/trends in surface temperature and precipitation during the satellite era (1979–2012). Clim. Dyn. 46, 1091–1105. https://doi.org/10.1007/s00382-015-2634-x

Harrison, L., Funk, C., Peterson, P., 2019. Identifying changing precipitation extremes in Sub-Saharan Africa with gauge and 470 satellite products. Environ. Res. Lett. 14, 085007. https://doi.org/10.1088/1748-9326/ab2cae

Hersbach, H., Bell, B., Berrisford, P., Hirahara, S., Horányi, A., Muñoz-Sabater, J., Nicolas, J., Peubey, C., Radu, R., Schepers, D., Simmons, A., Soci, C., Abdalla, S., Abellan, X., Balsamo, G., Bechtold, P., Biavati, G., Bidlot, J., Bonavita, M., Chiara, G.D., Dahlgren, P., Dee, D., Diamantakis, M., Dragani, R., Flemming, J., Forbes, R., Fuentes, M., Geer, A., Haimberger, L., Healy, S., Hogan, R.J., Hólm, E., Janisková, M., Keeley, S., Laloyaux, P., Lopez, P., 475 Lupu, C., Radnoti, G., Rosnay, P. de, Rozum, I., Vamborg, F., Villaume, S., Thépaut, J.-N., 2020. The ERA5 global reanalysis. Q. J. R. Meteorol. Soc. 146, 1999–2049. https://doi.org/10.1002/qj.3803

Houze, R.A., 2012. Orographic effects on precipitating clouds. Rev. Geophys. 50. https://doi.org/10.1029/2011RG000365

Howard, E., Washington, R., 2019. Drylines in Southern Africa: Rediscovering the Congo Air Boundary. J. Clim. 32, 8223–8242. https://doi.org/10.1175/JCLI-D-19-0437.1

480 Howard, E., Washington, R., 2018. Characterizing the Synoptic Expression of the Angola Low. J. Clim. 31, 7147–7165. https://doi.org/10.1175/JCLI-D-18-0017.1

IPCC, 2013. Annex I: Atlas of Global and Regional Climate Projections, in: Stocker, T.F., Qin, D., Plattner, G.-K., Tignor, M., Allen, S.K., Boschung, J., Nauels, A., Xia, Y., Bex, V., Midgley, P.M. (Eds.), Climate Change 2013: The Physical Science Basis. Contribution of Working Group I to the Fifth Assessment Report of the Intergovernmental 485 Panel on Climate Change. Cambridge University Press, Cambridge, United Kingdom and New York, NY, USA, pp. 1311–1394. https://doi.org/10.1017/CBO9781107415324.029

Janowiak, J.E., 1988. An Investigation of Interannual Rainfall Variability in Africa. J. Clim. 1, 240–255. https://doi.org/10.1175/1520-0442(1988)001<0240:AIOIRV>2.0.CO;2

Kendall, M.G., 1948. Rank correlation methods, Rank correlation methods. Griffin, Oxford, England.

490 Kim, J., Waliser, D.E., Mattmann, C.A., Goodale, C.E., Hart, A.F., Zimdars, P.A., Crichton, D.J., Jones, C., Nikulin, G., Hewitson, B., Jack, C., Lennard, C., Favre, A., 2014. Evaluation of the CORDEX-Africa multi-RCM hindcast: systematic model errors. Clim. Dyn. 42, 1189–1202. https://doi.org/10.1007/s00382-013-1751-7

Kim, Y.-H., Min, S.-K., Zhang, X., Sillmann, J., Sandstad, M., 2020. Evaluation of the CMIP6 multi-model ensemble for climate extreme indices. Weather Clim. Extrem. 29, 100269. https://doi.org/10.1016/j.wace.2020.100269

495 Kula, N., Haines, A., Fryatt, R., 2013. Reducing Vulnerability to Climate Change in Sub-Saharan Africa: The Need for Better Evidence. PLoS Med. 10. https://doi.org/10.1371/journal.pmed.1001374

Laprise, R., de Elía, R., Caya, D., Biner, S., Lucas-Picher, P., Diaconescu, E., Leduc, M., Alexandru, A., Separovic, L., Canadian Network for Regional Climate Modelling and Diagnostics, 2008. Challenging some tenets of Regional Climate Modelling. Meteorol. Atmospheric Phys. 100, 3–22. https://doi.org/10.1007/s00703-008-0292-9

500 Le Coz, C., van de Giesen, N., 2020. Comparison of Rainfall Products over Sub-Saharan Africa. J. Hydrometeorol. 21, 553–596. https://doi.org/10.1175/JHM-D-18-0256.1

L'Heureux, M.L., Lee, S., Lyon, B., 2013. Recent multidecadal strengthening of the Walker circulation across the tropical Pacific. Nat. Clim. Change 3, 571–576. https://doi.org/10.1038/nclimate1840

Lorenz, C., Kunstmann, H., 2012. The Hydrological Cycle in Three State-of-the-Art Reanalyses: Intercomparison and Performance Analysis. J. Hydrometeorol. 13, 1397–1420. https://doi.org/10.1175/JHM-D-11-088.1

Lyon, B., Mason, S.J., 2007. The 1997–98 Summer Rainfall Season in Southern Africa. Part I: Observations. J. Clim. 20, 5134–5148. https://doi.org/10.1175/JCLI4225.1

Mabhaudhi, T., Mpandeli, S., Nhamo, L., Chimonyo, V.G.P., Nhemachena, C., Senzanje, A., Naidoo, D., Modi, A.T., 2018. Prospects for Improving Irrigated Agriculture in Southern Africa: Linking Water, Energy and Food. Water 10, 1881. https://doi.org/10.3390/w10121881

Maidment, R.I., Allan, R.P., Black, E., 2015. Recent observed and simulated changes in precipitation over Africa. Geophys. Res. Lett. 42, 8155–8164. https://doi.org/10.1002/2015GL065765

Maidment, R.I., Grimes, D., Allan, R.P., Tarnavsky, E., Stringer, M., Hewison, T., Roebeling, R., Black, E., 2014. The 30 year TAMSAT African Rainfall Climatology And Time series (TARCAT) data set. J. Geophys. Res. Atmospheres 119, 10,619-10,644. https://doi.org/10.1002/2014JD021927

Mann, H.B., 1945. Nonparametric Tests Against Trend. Econometrica 13, 245–259. https://doi.org/10.2307/1907187

Munday, C., Washington, R., 2018. Systematic Climate Model Rainfall Biases over Southern Africa: Links to Moisture Circulation and Topography. J. Clim. 31, 7533–7548. https://doi.org/10.1175/JCLI-D-18-0008.1

Munday, C., Washington, R., 2017. Circulation controls on southern African precipitation in coupled models: The role of the Angola Low. J. Geophys. Res. Atmospheres 122, 861–877. https://doi.org/10.1002/2016JD025736

Nikulin, G., Jones, C., Giorgi, F., Asrar, G., Büchner, M., Cerezo-Mota, R., Christensen, O.B., Déqué, M., Fernandez, J., Hänsler, A., van Meijgaard, E., Samuelsson, P., Sylla, M.B., Sushama, L., 2012. Precipitation Climatology in an Ensemble of CORDEX-Africa Regional Climate Simulations. J. Clim. 25, 6057–6078. https://doi.org/10.1175/JCLI-D-11-00375.1

Onyutha, C., 2018. Trends and variability in African long-term precipitation. Stoch. Environ. Res. Risk Assess. 32, 2721–2739. https://doi.org/10.1007/s00477-018-1587-0

Peterson, T.C., Manton, M.J., 2008. Monitoring Changes in Climate Extremes: A Tale of International Collaboration. Bull. Am. Meteorol. Soc. 89, 1266–1271.

Pichelli, E., Coppola, E., Sobolowski, S., Ban, N., Giorgi, F., Stocchi, P., Alias, A., Belušić, D., Berthou, S., Caillaud, C., Cardoso, R.M., Chan, S., Christensen, O.B., Dobler, A., de Vries, H., Goergen, K., Kendon, E.J., Keuler, K., Lenderink, G., Lorenz, T., Mishra, A.N., Panitz, H.-J., Schär, C., Soares, P.M.M., Truhetz, H., Vergara-Temprado, J., 2021. The first multi-model ensemble of regional climate simulations at kilometer-scale resolution part 2: historical and future simulations of precipitation. Clim. Dyn. https://doi.org/10.1007/s00382-021-05657-4

Pierce, D.W., Barnett, T.P., Santer, B.D., Gleckler, P.J., 2009. Selecting global climate models for regional climate change studies. Proc. Natl. Acad. Sci. 106, 8441–8446. https://doi.org/10.1073/pnas.0900094106

Pinto, I., Lennard, C., Tadross, M., Hewitson, B., Dosio, A., Nikulin, G., Panitz, H.-J., Shongwe, M.E., 2016. Evaluation and projections of extreme precipitation over southern Africa from two CORDEX models. Clim. Change 135, 655–668. https://doi.org/10.1007/s10584-015-1573-1

Reason, C.J.C., Jagadheesha, D., 2005. A model investigation of recent ENSO impacts over southern Africa. Meteorol. Atmospheric Phys. 89, 181–205. https://doi.org/10.1007/s00703-005-0128-9

Rocklöv, J., Dubrow, R., 2020. Climate change: an enduring challenge for vector-borne disease prevention and control. Nat. Immunol. 21, 479–483. https://doi.org/10.1038/s41590-020-0648-y

Sen, P.K., 1968. Estimates of the Regression Coefficient Based on Kendall's Tau. J. Am. Stat. Assoc. 63, 1379–1389. https://doi.org/10.1080/01621459.1968.10480934

Serdeczny, O., Adams, S., Baarsch, F., Coumou, D., Robinson, A., Hare, W., Schaeffer, M., Perrette, M., Reinhardt, J., 2017. Climate change impacts in Sub-Saharan Africa: from physical changes to their social repercussions. Reg. Environ. Change 17, 1585–1600. https://doi.org/10.1007/s10113-015-0910-2

Tarnavsky, E., Grimes, D., Maidment, R., Black, E., Allan, R.P., Stringer, M., Chadwick, R., Kayitakire, F., 2014. Extension of the TAMSAT Satellite-Based Rainfall Monitoring over Africa and from 1983 to Present. J. Appl. Meteorol. Climatol. 53, 2805–2822. https://doi.org/10.1175/JAMC-D-14-0016.1

Taylor, K.E., Stouffer, R.J., Meehl, G.A., 2012. An Overview of CMIP5 and the Experiment Design. Bull. Am. Meteorol. Soc. 93, 485–498. https://doi.org/10.1175/BAMS-D-11-00094.1

Theil, H., 1992. A Rank-Invariant Method of Linear and Polynomial Regression Analysis, in: Raj, B., Koerts, J. (Eds.), Henri Theil's Contributions to Economics and Econometrics: Econometric Theory and Methodology, Advanced Studies in Theoretical and Applied Econometrics. Springer Netherlands, Dordrecht, pp. 345–381. https://doi.org/10.1007/978-94-011-2546-8_20

Tirado, M.C., Hunnes, D., Cohen, M.J., Lartey, A., 2015. Climate Change and Nutrition in Africa. J. Hunger Environ. Nutr. 10, 22–46. https://doi.org/10.1080/19320248.2014.908447

Toté, C., Patricio, D., Boogaard, H., Van der Wijngaart, R., Tarnavsky, E., Funk, C., 2015. Evaluation of Satellite Rainfall Estimates for Drought and Flood Monitoring in Mozambique. Remote Sens. 7, 1758–1776. https://doi.org/10.3390/rs70201758

Ukkola, A.M., Kauwe, M.G.D., Roderick, M.L., Abramowitz, G., Pitman, A.J., 2020. Robust Future Changes in Meteorological Drought in CMIP6 Projections Despite Uncertainty in Precipitation. Geophys. Res. Lett. 47, e2020GL087820. https://doi.org/10.1029/2020GL087820

Warnatzsch, E.A., Reay, D.S., 2019. Temperature and precipitation change in Malawi: Evaluation of CORDEX-Africa climate simulations for climate change impact assessments and adaptation planning. Sci. Total Environ. 654, 378–392. https://doi.org/10.1016/j.scitotenv.2018.11.098

Wyser, K., van Noije, T., Yang, S., von Hardenberg, J., O'Donnell, D., Döscher, R., 2020. On the increased climate sensitivity in the EC-Earth model from CMIP5 to CMIP6. Geosci. Model Dev. 13, 3465–3474. https://doi.org/10.5194/gmd-13-3465-2020

Yim, B.Y., Yeh, S.-W., Sohn, B.-J., 2016. ENSO-Related Precipitation and Its Statistical Relationship with the Walker Circulation Trend in CMIP5 AMIP Models. Atmosphere 7, 19. https://doi.org/10.3390/atmos7020019

575
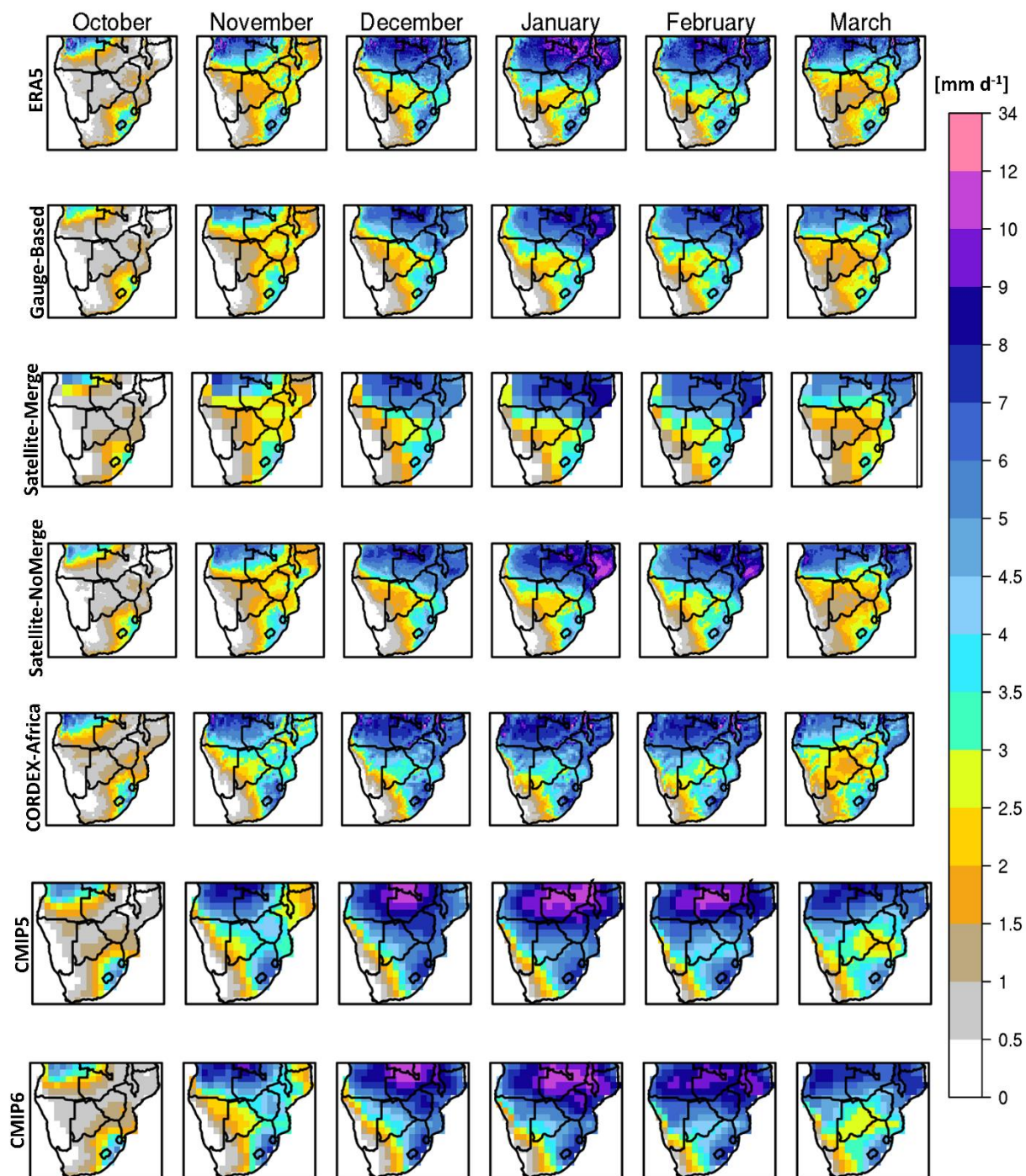
Figure 1. Monthly precipitation climatologies during the period 1986-2005 in mm d⁻¹. More specifically, from top to bottom: ERA5 reanalysis dataset. Gauge-based: Ensemble mean of datasets that were produced by employing spatial interpolation methods using rain gauges/station data. Satellite-Merge: Ensemble mean of all satellite products that merge with rain gauges/station data. Satellite-NoMerge: Ensemble mean of satellite products that do not merge with rain
580 gauges/station data. CORDEX-Africa: Ensemble mean of regional climate model simulations performed in the context of Coordinated Regional Climate Downscaling Experiment (CORDEX) – Africa domain. CMIP5: Ensemble mean of general circulation models participating in the Coupled Model Intercomparison Project Phase 5 (CMIP5) that were used as forcing in the CORDEX-Africa simulations. CMIP6: Ensemble mean of general circulation models participating in the Coupled Model Intercomparison Project Phase 6.

Figure 2. Standard deviation of monthly precipitation [mm d⁻¹] during the period 1986-2005. Rows indicate the ensemble means analyzed. More specifically, from top to bottom: Gauge-based: Ensemble mean of datasets that were produced by employing spatial interpolation methods using rain gauges/station data. Satellite-Merge: Ensemble mean of all satellite products that merge with rain gauges/station data. Satellite-NoMerge: Ensemble mean of satellite products that do not merge with rain gauges/station data. CORDEX-Africa: Ensemble mean of regional climate model simulations performed in the context of Coordinated Regional Climate Downscaling Experiment – Africa domain. CMIP5: Ensemble mean of general circulation models participating in the Coupled Model Intercomparison Project Phase 5 (CMIP5) that were used as forcing in

the CORDEX-Africa simulations. CMIP6: Ensemble mean of general circulation models participating in the Coupled Model Intercomparison Project Phase 6.

595

600

605

610

615
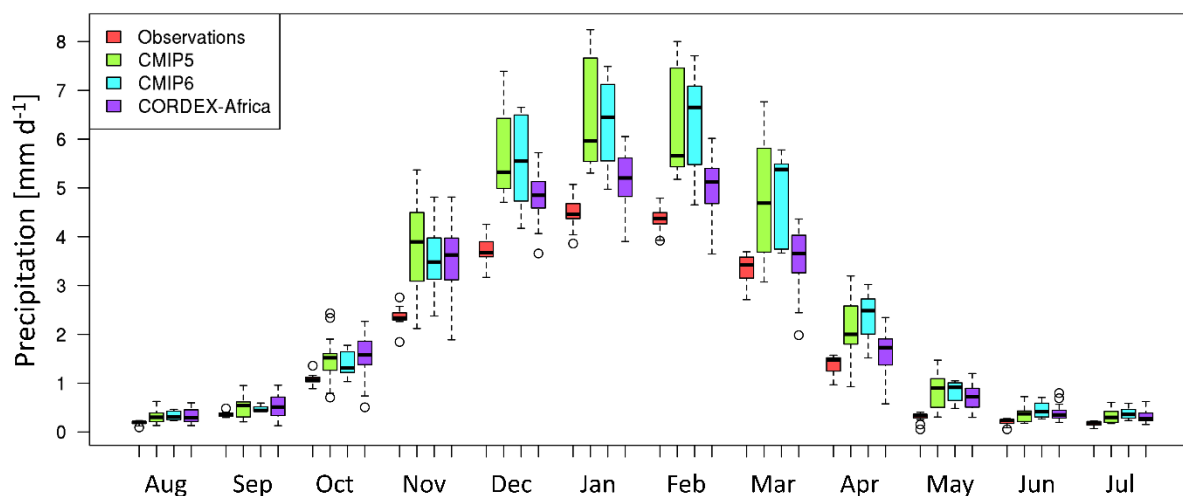
Figure 3. Annual cycle of monthly precipitation during 1986-2005 for the ensemble of observational data (gauge-based, satellite and reanalysis), CMIP5 (Coupled Model Intercomparison Project Phase 5), CMIP6 (Coupled Model Intercomparison Project Phase 6) and CORDEX-Africa (Coordinated Regional Climate Downscaling Experiment – Africa domain). The thick horizontal black lines indicate the ensemble median for each month, the box encloses the interquartile range, and the tails denote the full ensemble range. Circles represent the outliers for each ensemble. Grid points only are considered.
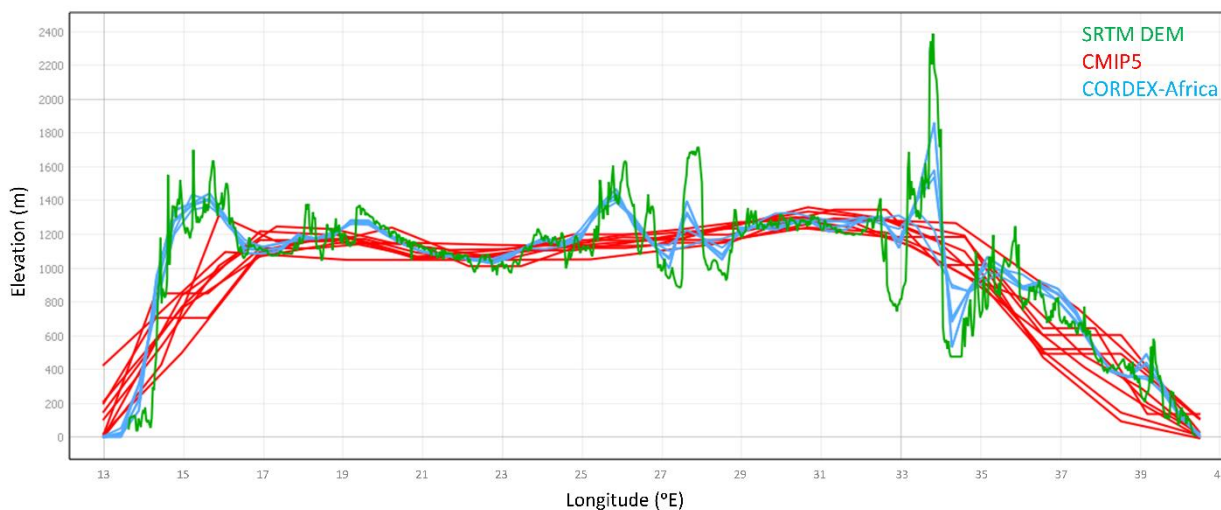
Figure 4. Cross section of surface elevation at 10.5 °S across southern Africa for the Shuttle Radar Topography Mission (SRTM) Digital Elevation Model (in green), the surface altitude as represented in the CMIP5 (Coupled Model Intercomparison Project Phase 5) global climate models (in red) and the surface elevation as represented in the CORDEX-Africa (Coordinated Regional Climate Downscaling Experiment – Africa domain) regional climate models (in blue).
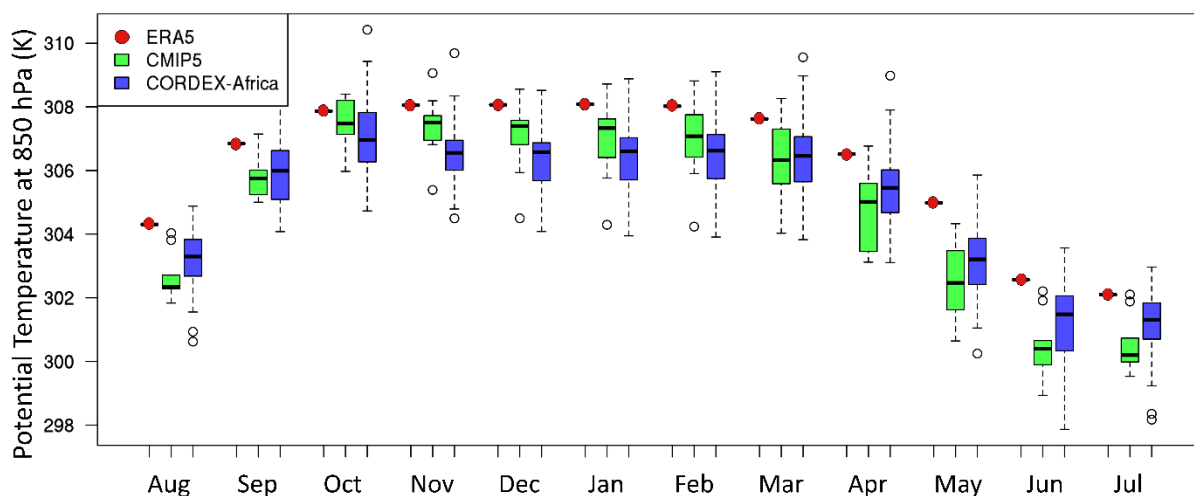
Figure 5. Annual cycle of potential temperature at 850 hPa (theta850) during 1986-2005 for the CMIP5 (Coupled Model Intercomparison Project Phase 5) and CORDEX-Africa CORDEX-Africa (Coordinated Regional Climate Downscaling Experiment– Africa domain) ensembles. The thick horizontal black lines indicate the ensemble median for each month, the box encloses the interquartile range, and the tails denote the full ensemble range. Circles represent the outliers for each ensemble. Red dot represents theta850 from ERA5. Temperature in CMIP6 was not available at 850 hPa, hence theta850 was not calculated for CMIP6. Grid points only are considered.
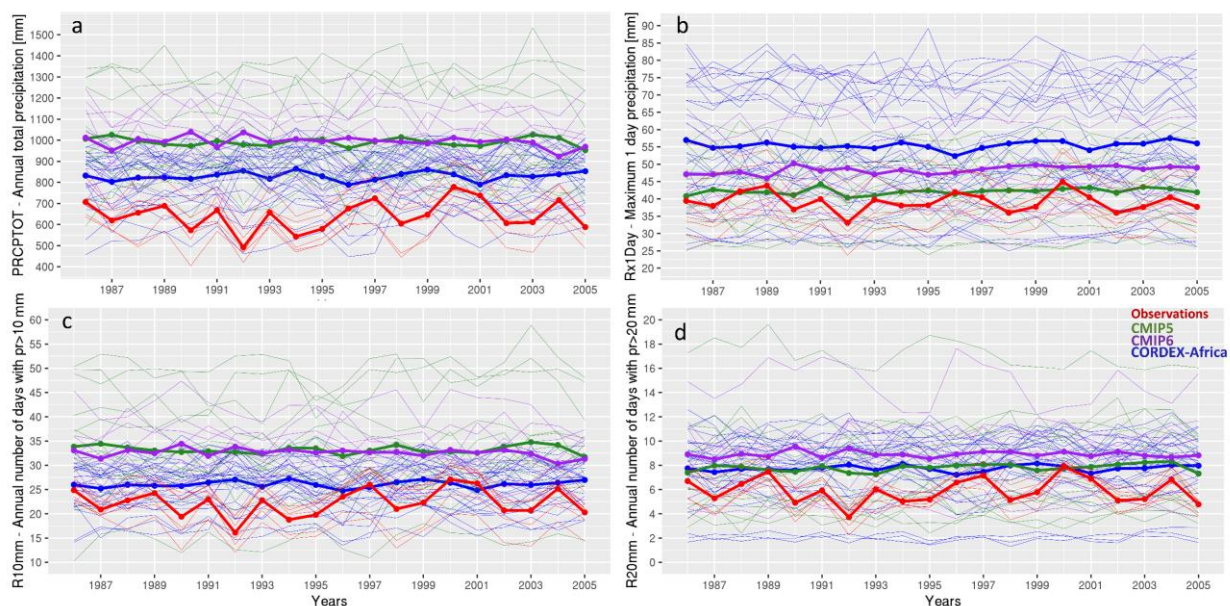
Figure 6. Timeseries of the ETCCDI indices over southern Africa (10 ºE to 42 ºE and 10 ºS to 35 ºS) for the observational ensemble in red (gauge-based, satellite and reanalysis), CMIP5 (Coupled Model Intercomparison Project Phase 5) ensemble

in green, CMIP6 (Coupled Model Intercomparison Project Phase 6) ensemble in purple and CORDEX-Africa (Coordinated Regional Climate Downscaling Experiment – Africa domain) ensemble in blue. Thin lines display single ensemble members, thick lines display ensemble means. Y-axis on each panel depicts: (a) PRCPTOT (total annual precipitation), (b) Rx1Day
645   (annual maximum daily precipitation), (c) R10mm (annual number of days with daily precipitation >10 mm), (d) R20mm (annual number of days with daily precipitation >20 mm).
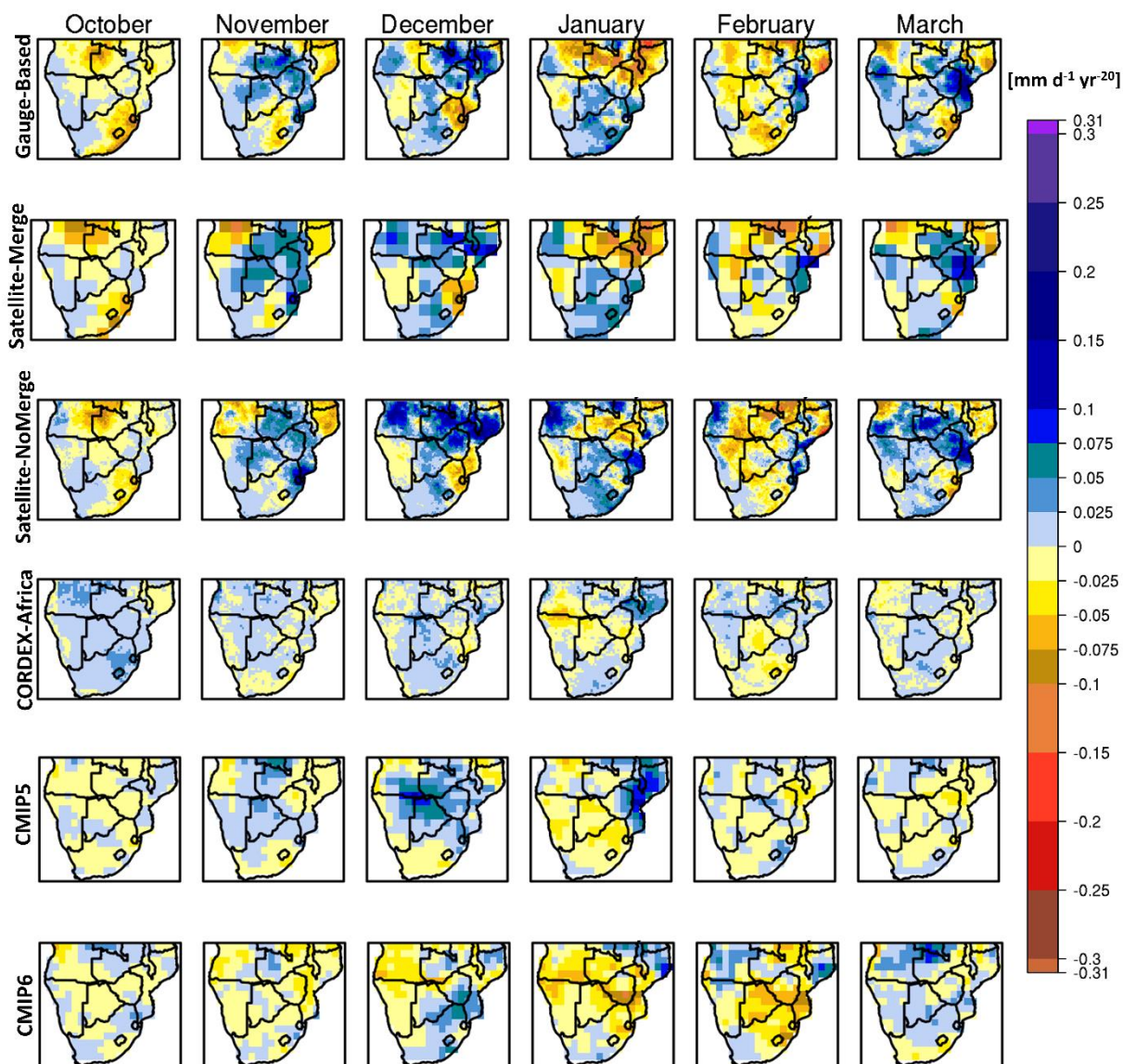
Figure 7. Trends for monthly precipitation for the period 1986-2005 [mm d^{-1} per 20 years] calculated using Sen's Slope. Rows indicate the ensemble mean of trends produced by each ensemble member. More specifically, from top to bottom:

650   Gauge-Based: Ensemble mean of datasets that were produced by employing spatial interpolation methods using rain gauges/station data. Satellite-Merge: Ensemble mean of all satellite products that merge with rain gauges/station data. Satellite-NoMerge: Ensemble mean of satellite products that do not merge with rain gauges/station data. CORDEX-Africa: Ensemble mean of regional climate model simulations performed in the context of Coordinated Regional Climate Downscaling Experiment – Africa domain. CMIP5: Ensemble mean of general circulation models participating in the

655   Coupled Model Intercomparison Project Phase 5 (CMIP5) that were used as forcing in the CORDEX-Africa simulations. CMIP6: Ensemble mean of general circulation models participating in the Coupled Model Intercomparison Project Phase 6.